

MODIFICATIONS TO THE VV PHTS RELAP5 MODEL

December 2010

This report was prepared as an account of work sponsored by an agency of the United States Government. Neither the United States Government nor any agency thereof, nor any of their employees, makes any warranty, express or implied, or assumes any legal liability or responsibility for the accuracy, completeness, or usefulness of any information, apparatus, product, or process disclosed, or represents that its use would not infringe privately owned rights. Reference herein to any specific commercial product, process, or service by trade name, trademark, manufacturer, or otherwise, does not necessarily constitute or imply its endorsement, recommendation, or favoring by the United States Government or any agency thereof. The views and opinions of authors expressed herein do not necessarily state or reflect those of the United States Government or any agency thereof.

MODIFICATIONS TO THE VV PHTS RELAP5 MODEL


Juan J. Carbajo

Date Published: December 2010

Prepared by
OAK RIDGE NATIONAL LABORATORY
Oak Ridge, Tennessee 37831-6283
managed by
UT-BATTELLE, LLC
for the
U.S. DEPARTMENT OF ENERGY
under contract DE-AC05-00OR22725

MODIFICATIONS TO THE VV PHTS RELAP5 MODEL


December 2010



Graydon L. Yoder, Jr.
Group Leader, Thermal Hydraulics & Irradiation Engineering

1/28/11

Date



Jan B. Berry
WBS Team Leader, U.S. ITER Cooling Water System

1/31/11

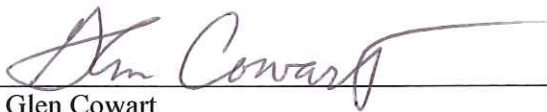
Date



Brad Nelson
Chief Engineer, U.S. ITER

2/2/11

Date



Glen Cowart
QA Specialist, U.S. ITER

2/4/2011

Date

CONTENTS

	Page
LIST OF FIGURES	vii
LIST OF TABLES	ix
ACRONYMS	xi
ABSTRACT	1
1. INTRODUCTION	1
2. PUMP MODELS	1
3. STEAM PRESSURIZER	1
4. COOLANT WATER TEMPERATURE CONTROLS.....	3
5. PULSED-POWER INPUT VALUES	3
6. PIPE STRUCTURES	5
7. RESULTS FOR PULSED-POWER OPERATION WITH THE NEW MODEL.....	5
8. RESULTS FOR BAKING OPERATION	5
9. DECAY HEAT MODEL.....	10
10. REFERENCES	10

LIST OF FIGURES

Figure		Page
1	RELAP5 nodalization of the VV PHTS RELAP5 model.....	4
2	Primary system valve temperature controls. Reference temperature is 100°C.....	4
3	Powers deposited into the coolant and removed by the HX.	6
4	Plasma pulsed power deposited into the VV walls.....	6
5	Water temperatures entering and leaving the VV.....	7
6	Heater power during the complete baking transient.	8
7	Heater power at the beginning of the baking transient.	8
8	Temperatures during the complete baking transient.	9
9	Temperatures during the first 1000 s of the baking transient.	9
10	Temperatures at the end of the baking transient.	10

LIST OF TABLES

Table		Page
1	Pressurizer specifications.....	2
2	Pressurizer model hydraulic data.....	2
3	Pressurizer heat structures.....	3

ACRONYMS

HX	heat exchanger
FW/BLK	First Wall/Blanket
PHTS	Primary Heat Transfer System
PI	proportional integral
VV	Vacuum Vessel

ABSTRACT

Modifications and improvements to a previous RELAP5 model of the Vacuum Vessel Primary Heat Transfer System are described in this report. The modifications were new pump models, a new steam pressurizer, new coolant water control systems, additional pipe structures, and reduction of the pulse power to 6 MW.

1. INTRODUCTION

A RELAP5 model of the Vacuum Vessel (VV) Primary Heat Transfer System (PHTS) was prepared and described previously in Ref. 1. This report documents modifications and improvements to that model. These modifications included new pump models replacing the previous ones, a steam pressurizer replacing the gas one, the cooling water temperature control system being moved to the primary system from the secondary one, addition of structures modeling the mass of steel in the pipes, and finally, the power pulses being reduced to 6 MW from 10 MW without changing the duration of pulse power and dwell times. Some results with the new RELAP5 model are also presented.

2. PUMP MODELS

Two new pump models have been implemented—one for the main pump in the main loop and the other for the decay heat pump in the decay heat/safety loop.

The new main pump model is based on the model employed in Ref. 2, modified for the flow and head required in the VV PHTS. The pump uses Westinghouse built-in data. The pump supplies 950 kg/s ($\sim 1 \text{ m}^3/\text{s}$) of water flow at 0.8 MPa, with a pump speed of 1450 rpm (151.8 rad/s), rated pump head of 84 m, rated pump torque of 5,968 N.m, and moment of inertia of $420 \text{ kg}\cdot\text{m}^2$. The pump efficiency is 0.85. The pump head and flow rate were based on the required VV flow and the system's overall pressure drop. The pump efficiency of 85% was an assumed value that then dictated the pump torque. The pump speed was an assumed value, and the moment of inertia was scaled from Ref. 2.

The pump model for the decay heat loop provides 40 kg/s, with a pump speed of 1450 rpm (151.8 rad/s), rated pump head of 70.5 m, rated pump torque of 825 N.m, moment of inertia $18 \text{ kg}\cdot\text{m}^2$, and pump efficiency of 0.85. These values were developed in a similar fashion to those for the main pump. The pump uses Westinghouse built-in data like the main pump model.

3. STEAM PRESSURIZER

The steam pressurizer model is also based in the model of Ref. 2, with water spray injection and two heaters. The total volume of the previous gas pressurizer was 40 m^3 to accommodate volume changes between 20 and 200°C . A volume control tank is assumed to be used to accommodate the volume change. Therefore, the VV pressure can be controlled using a smaller steam pressurizer (volume of 16.7 m^3 , as in Ref. 2). Table 1 shows the pressurizer specifications.

Table 1. Pressurizer specifications*

Item	Specification
Type	Steam pressurizer
Total internal volume, m ³	16.7
Free volume, m ³	8 (nominal)
Inside diameter, m	1.9
Thickness of shell, mm	50
Length of shell, m	6.7
Major structural material	Type 304L stainless steel
Design pressure, MPa	2.5
Design temperature, °C	240
Approximate mass, ton	30
Heater power, kW	120 (proportional) 300 (backup)
Flow rate of water splay, kg/s	0.04 (continuous) 1.0 (maximum during pulse)

*These design specification are to be verified and optimized by the Tokamak Cooling Water System designer during the preliminary design.

The pressurizer has two heaters, rated at 120 and 300 kW, and one spray system, as indicated in Table 1. Table 2 shows the hydraulic components used in RELAP5-3D to model the pressurizer. Table 3 shows the heat structures used in RELAP5-3D to model the pressurizer walls and the two heaters. Control systems for the heaters and spray are also included in the model. The pressurizer pressure is set at 0.42 MPa to ensure 0.8 MPa at the VV inlet. The power of the heaters and the flow of the spray were taken from the pressurizer of Ref. 2, which was designed for the First Wall/Blanket (FW/BLK) PHTS. The requirements for the VV PHTS pressurizer are different from those used in the FW/BLK PHTS; therefore, some of the specifications of this pressurizer may have to be revised and changed.

Table 2. Pressurizer model hydraulic data

Component number and type	Component function	Number of cells	Overall length (m)	Volume (L)	Hydraulic diameter (mm)	Total pressure loss factors
340—branch	Surge line	39	10.15	27.7	59	1.25
341—pipe	PRZ bottom	10	0.95	1,796	—	—
343—pipe	PRZ vessel	40	4.62	13,100	—	—
344—branch	PRZ dome	1	0.95	1,796	—	—

PRZ = pressurizer

Table 3. Pressurizer heat structures

Structure number	Component function	Left thermal condition	Right thermal condition	Overall length (m)	Area (m ²)	Thickness (mm)	Material
9540	PRZ bottom	Pipe-341	90 W/m ²	Sphere	2.0	30	SS 316
9560	PRZ vessel	Pipe-343	90 W/m ²	4.58	30.0	50	SS 316
9580	PRZ dome	Branch-344	90 W/m ²	Sphere	2.0	30	SS 316
<i>Modeling information for PRZ heaters</i>							
9541	Proportional heater	—	Pipe-341	0.95	0.5	11	Ni-Cr
9542	Backup heater	—	Pipe-341	0.95	25.1	11	Ni-Cr

PRZ = pressurizer

4. COOLANT WATER TEMPERATURE CONTROLS

The temperature of the water coolant entering the VV is controlled by mixing cold water leaving the heat exchanger (HX) with hot water that bypasses it. The two valves that are active for this control are valve 228, downstream of the main HX (CV-222) in Fig. 1, and valve 261 in the bypass line, located at the bottom right corner of Fig. 1. These valves were in the original model but were changed to motor-operated valves with control systems (servo valves in RELAP5 nomenclature), and additional controls have been added. Control systems were taken from Ref. 2 with some simplifications. The reference temperature is 100°C (373 K). Figure 2, taken from Ref. 2, is a schematic of this control system. The cold-leg temperature reading from control volume 100 of Fig. 1 (downstream of the pump) is compared to a temperature target set point (100°C) in a proportional integral (PI) controller, and an error is produced. After introducing a dead band of 5% and scaling down the value within the range 0–1 in component 54, the resultant signal is compared to the valve’s current position. An error signal regarding the position of the valve is generated that triggers an impulse to either open or close the valve if larger (positive or negative) than 1%. This last impulse is again scaled so as to give an opening time of the valve of 27 s with constant rate (0.0371/s). It is continuously integrated, and the resultant function is the valve opening area. A simplified model has also been implemented as an alternative control system. The previous control systems in the secondary side of the main HX using trip valves 404 and 409 (top left corner of Fig. 1) were deactivated.

5. PULSED-POWER INPUT VALUES

Plasma pulsed power has been reduced from 10 MW/pulse to 6 MW/pulse with the same pulse duration: 30 s ramp up, 60 s ramp down, and 400 s plasma period. Each cycle repeats every 1800 s, unchanged from the previous cycle duration. This lower pulse power should reduce the HX cooling requirements. The average power during a complete cycle (1800 s) is now

$$P = 6[400 + (30 + 60)/2]/1800 = 1.483 \text{ MW.}$$

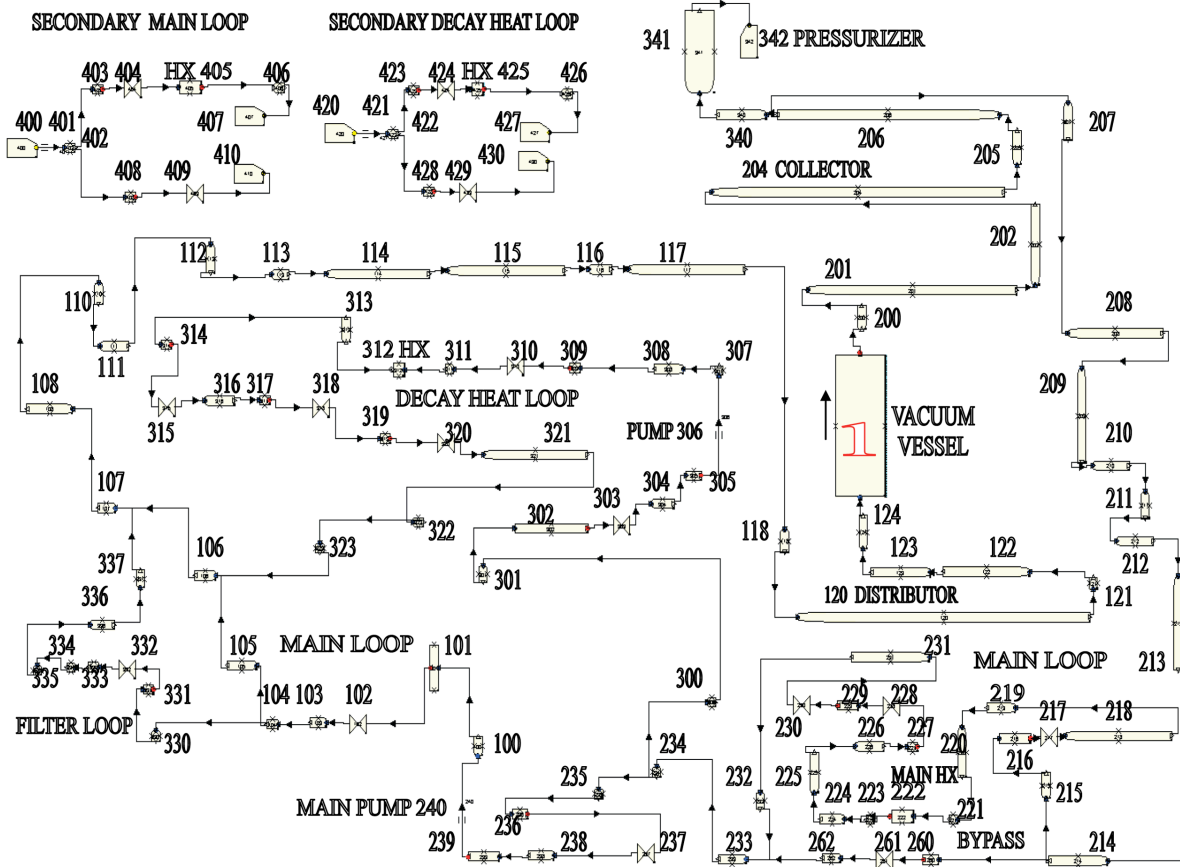


Fig. 1. RELAP5 nodalization of the VV PHTS RELAP5 model. (Figure taken from Ref. 1.)

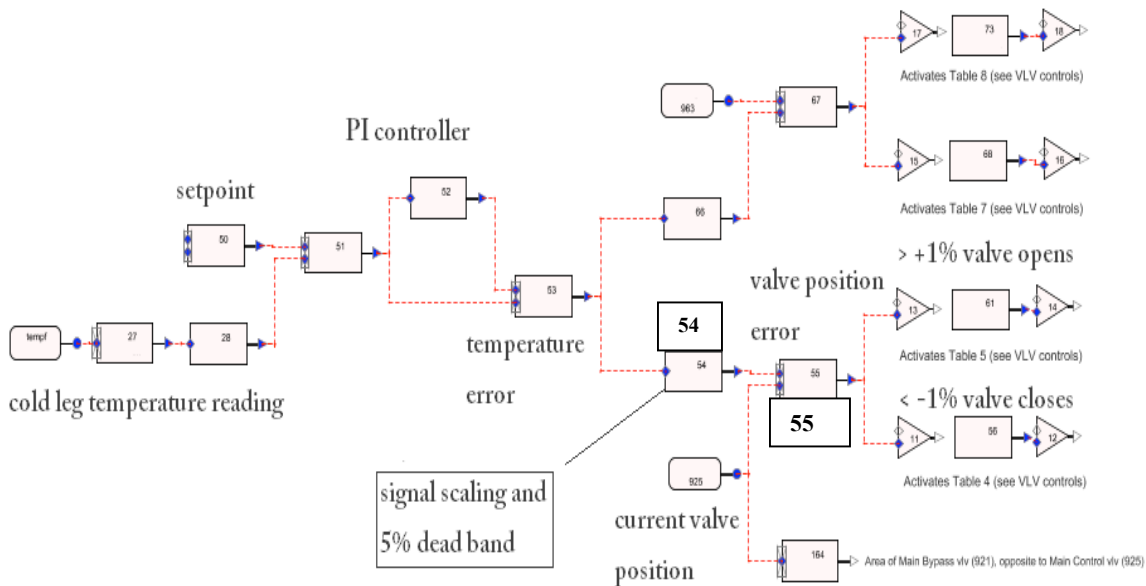


Fig. 2. Primary system valve temperature controls. Reference temperature is 100°C. (Figure taken from Ref. 2.)

6. PIPE STRUCTURES

The mass of the pipes has been modeled in RELAP5 as cylindrical structures surrounding the different hydraulic volumes that model the different pipes of the VV PHTS. It was assumed that the pipes are stainless steel Schedule 40S. Different pipe sizes are employed in the RELAP5 model. The main pipe is 16 in. (400 mm) in diameter; the wall thickness of this pipe was taken as 0.375 in. or 9.53 mm. (Most references do not have 16 in. pipe Schedule 40S reported; the wall thickness reported for regular Schedule 40 is larger: 0.5 in. or 12.7 mm.) The collector and distributor ring headers consist of 14 in. (350 mm) pipe, and the same wall thickness as for the 16 in. pipe (0.375 in. or 9.53 mm) was used. For 6 in. pipe, a wall thickness of 0.28 in. or 7.12 mm was used. For the 5 in. pipe, the thickness used was 0.258 in. (6.56 mm), and finally, for the 4 in. pipes, a thickness of 0.237 in. or 6.02 mm was used. These pipe structures are used in the baking model because the structures need to be heated together with the water circulating inside the piping.

7. RESULTS FOR PULSED-POWER OPERATION WITH THE NEW MODEL

RELAP5 calculations for pulsed-power operation of the VV PHTS were completed, and some of the results are presented here. The new model incorporates the new main pump model, a steam pressurizer, primary system temperature controls, reduced pulsed power (6 MW per pulse), and the pipe structures. Because of the lower pulse power, a lower-capacity HX is needed. The HX capacity can be varied by varying the secondary flow of water. The water flow in the secondary system was decreased from the value of 25.2 kg/s used in the previous model of Ref. 1 to a lower value of 17.8 kg/s. This HX secondary mass flow rate of 17.8 kg/s was kept constant during the complete transient calculation (10,000 s). There are no controls in this model for the secondary mass flow rate of cooling water. The new cooling load of the HX is ~2.56 MW, while in the previous model the cooling load was ~3.5 MW. Because the average power of the pulses is 1.48 MW (as calculated in Sect. 5), the HX removes the average pulsed power plus the pump power, which is estimated at 1.08 MW. Figure 3 shows the power deposited by the VV walls into the coolant, the power deposited into the coolant by the main pump, and the power removed by the HX, which is the sum of the two previous powers. Figure 4 shows the pulsed power used in this calculation during 10,000 s time—six peak pulses of 6 MW, with each cycle being 1800 s. This pulsed power is deposited directly into the walls of the VV, and the power is transferred from the VV walls into the coolant as shown in Fig. 3. Figure 5 shows the coolant water temperature into the VV (cold) and out of it (hot). The control systems of the HX did not have to operate in this calculation because the cold water temperature was not below the set point of 100°C. The bypass valve (V-261) was closed all the time, the valve at the exit of the HX (V-228) was fully open all the time, and no mixing of cool and hot water took place. Calculations with a larger cooling load on the HX have been completed to check that the bypass valve opens when the cold water temperature is below 100°C.

8. RESULTS FOR BAKING OPERATION

Given that the new pump model generates different amounts of power that are eventually released into the system coolant, calculation for the baking operation with the pipe structures was performed with the old pump model to compare this calculation *with structures* to the previous baking calculation *without structures*.

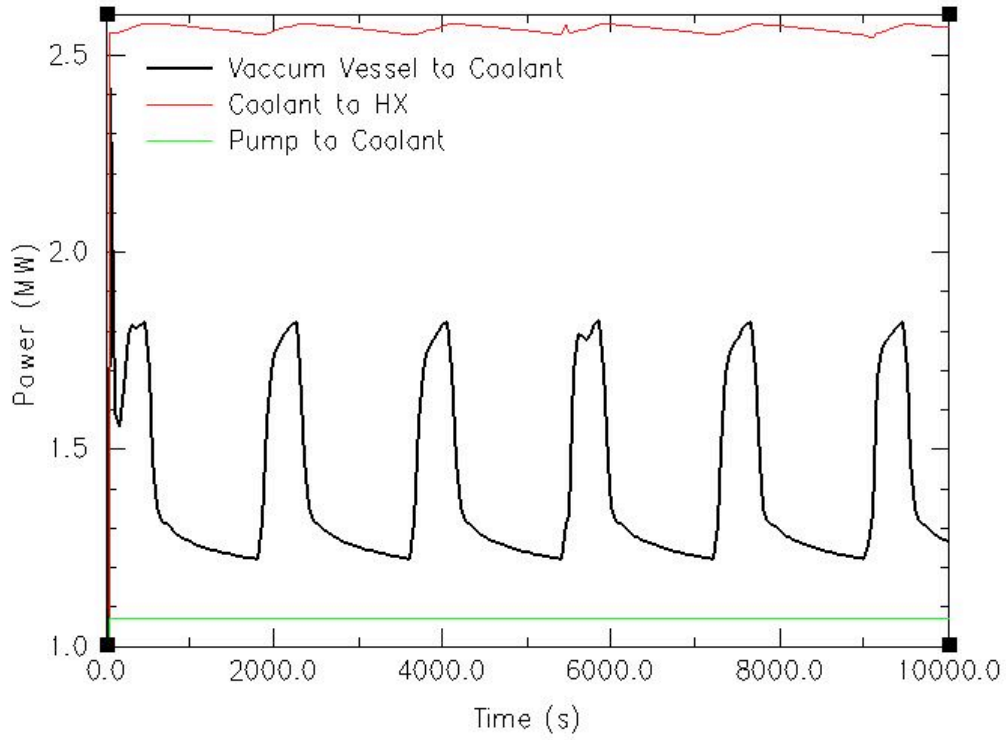


Fig. 3. Powers deposited into the coolant and removed by the HX.

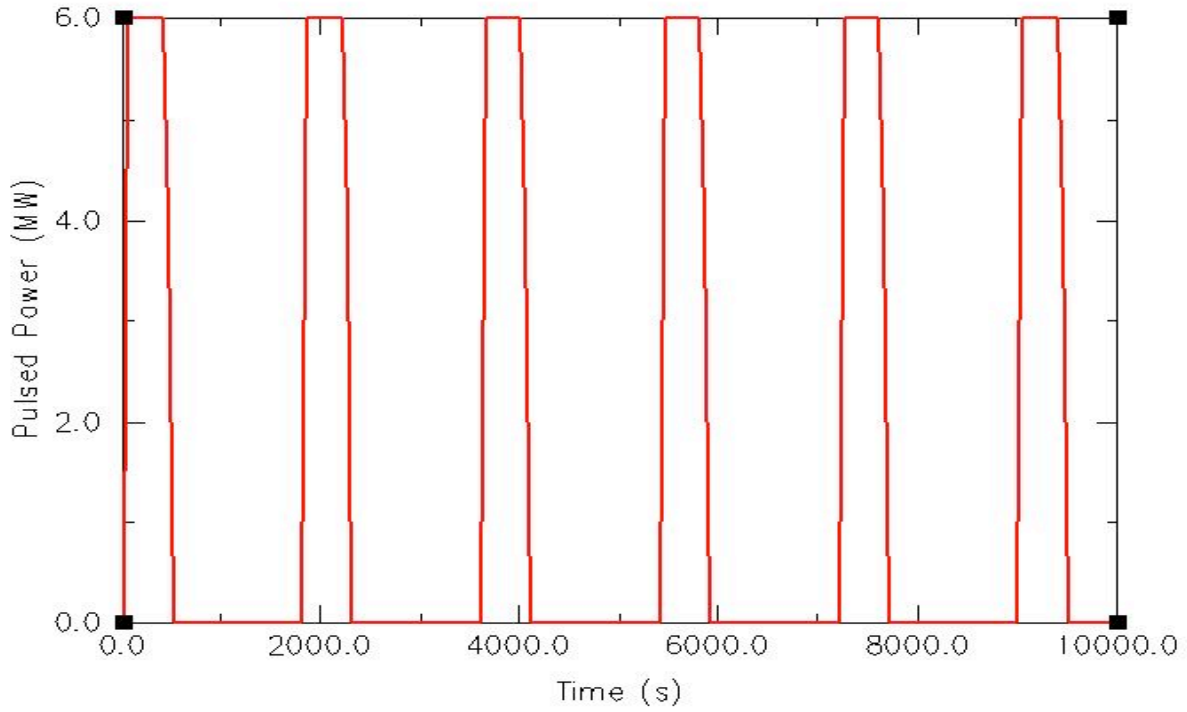


Fig. 4. Plasma pulsed power deposited into the VV walls.

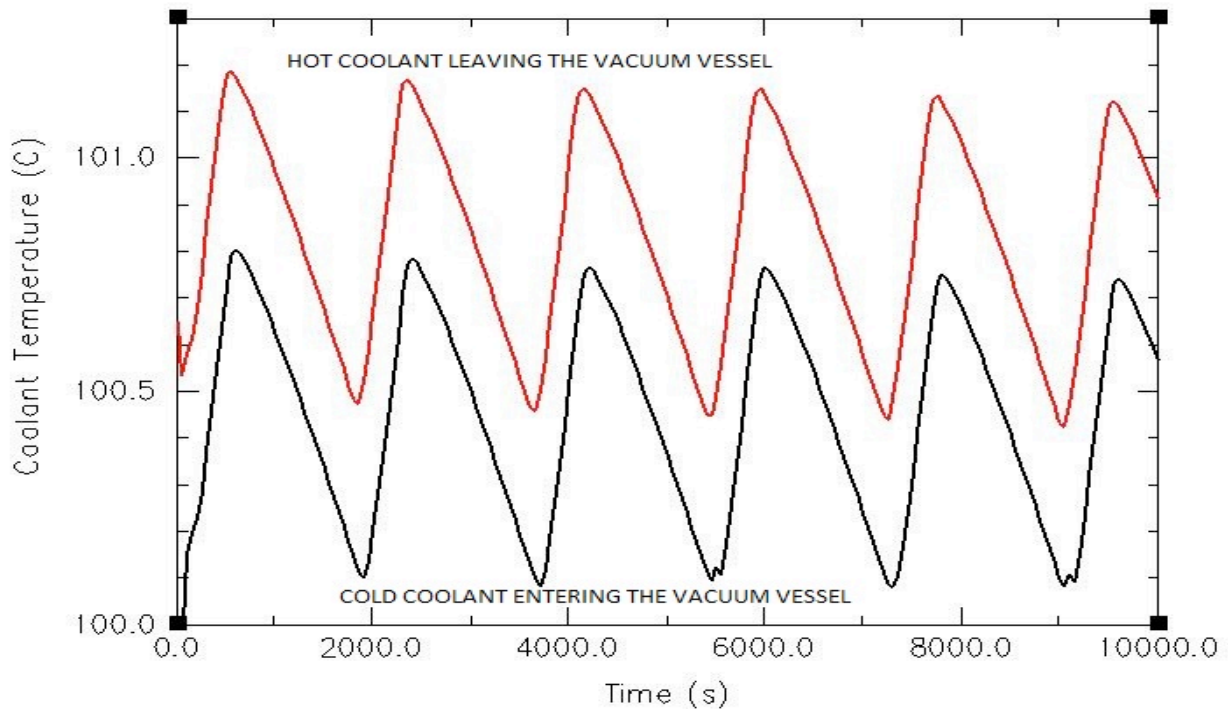


Fig. 5. Water temperatures entering and leaving the VV.

The power of the heater required for this baking operation is 3.04 MW, which is 0.03 MW (30 kW) greater than the heater power needed in the previous model without the structures of the pipes. Thus, the mass of the pipe structures does not significantly increase the heating capacity of the system. Still, heat losses to the environment were not accounted for, and if heat losses take place, more power will be required for the heater.

The same conditions employed in the previous baking calculation were employed here, so the results from the two calculations can be compared. These conditions are pump flow of 500 kg/s, system pressure of 2.4 MPa at the VV inlet, initial temperature of the system at 20°C (293 K), and final temperature of the system at 200°C (473 K). The main HX was disconnected from this model, and a heater was added to the cold leg. The temperature-increase rate is required to be less than 5°C/h anywhere in the system (in any structure of the VV, but not in the water). The power of the heater was gradually increased at the beginning of the transient until 490 s; beginning at this time, full power was maintained until the end of the transient. The power was gradually reduced to zero at the end of the transient. Figure 6 shows the power of the heater during the complete transient. Figure 7 shows the power of the heater at the beginning of the transient; full heater power of 3.04 MW was kept after 490 s. With these conditions, the final temperature of 200°C (473 K) was achieved in 134,000 s or 27.2 h, which is less than the maximum allowed time of 48 h.

Figures 8, 9, and 10 show the temperatures calculated by RELAP5 during the baking operation. Temperatures shown are for the hot water entering the VV, the cooler water leaving the VV, and the VV steel structure at two positions: bottom or lowest VV level (where the hot water enters the VV) and top or highest VV level (where the water leaves the VV). Figure 9 shows the temperatures at the beginning of the heating operation and Fig. 10 at the end of the heating. Two temperatures are shown for each VV structure: *surface*—in contact with the water—and *average*—average temperature of the structure. The temperature of the VV wall never goes above 200°C.

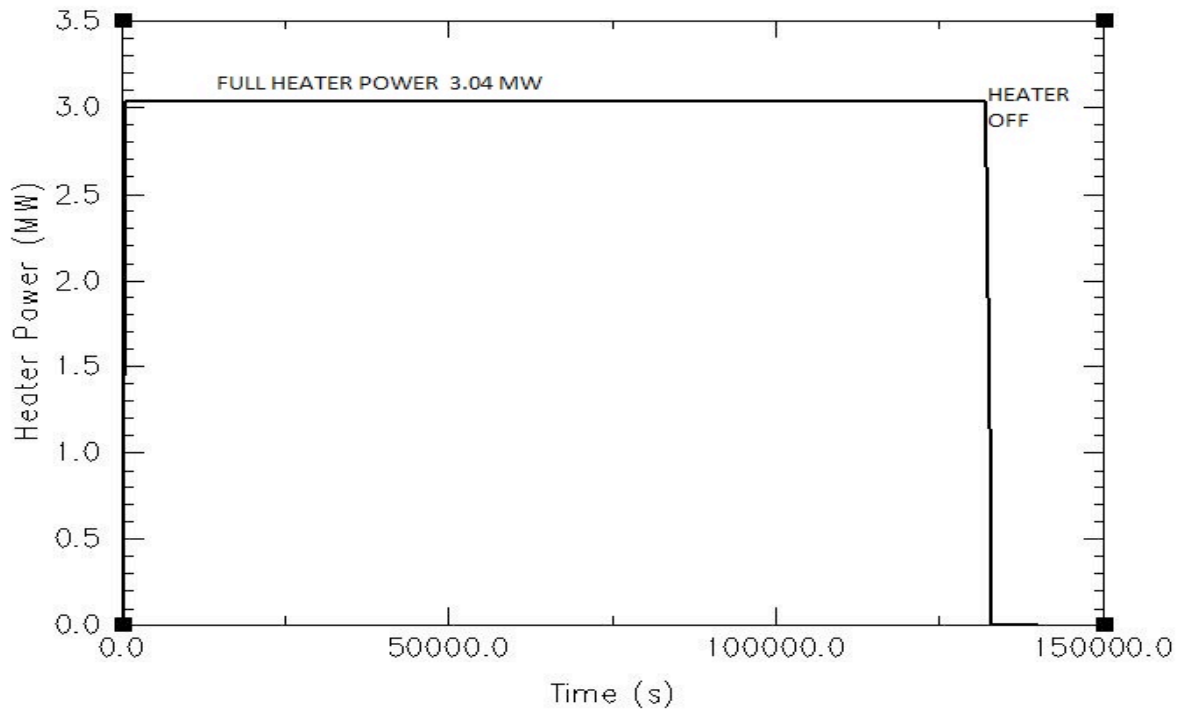


Fig. 6. Heater power during the complete baking transient.

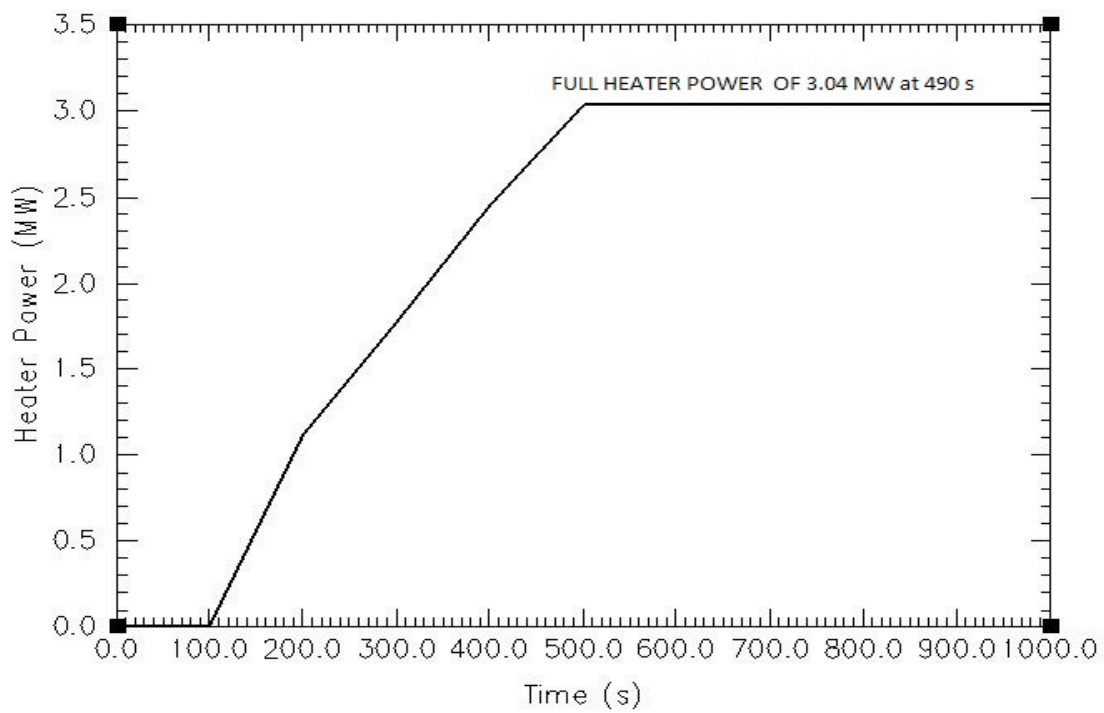


Fig. 7. Heater power at the beginning of the baking transient.

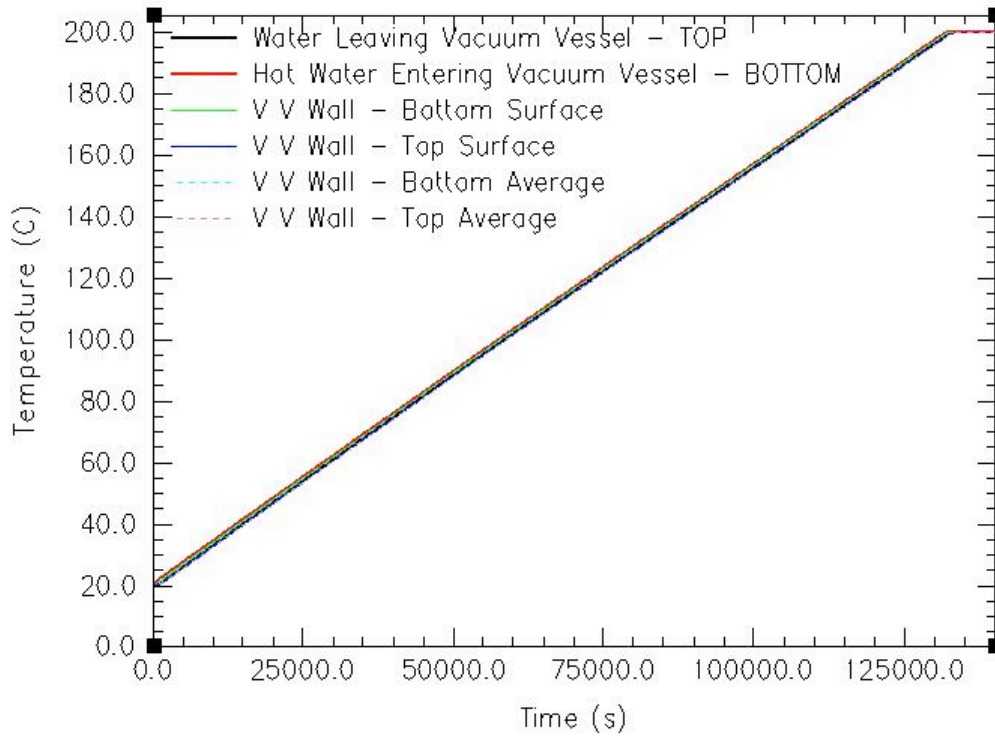


Fig. 8. Temperatures during the complete baking transient.

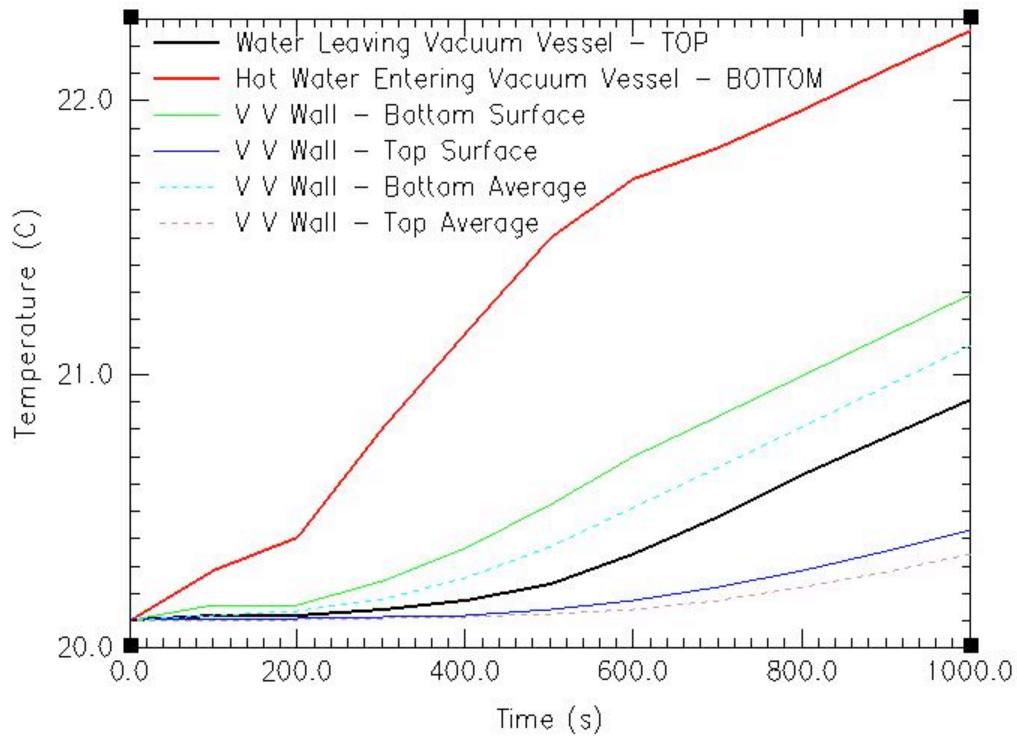


Fig. 9. Temperatures during the first 1000 s of the baking transient.

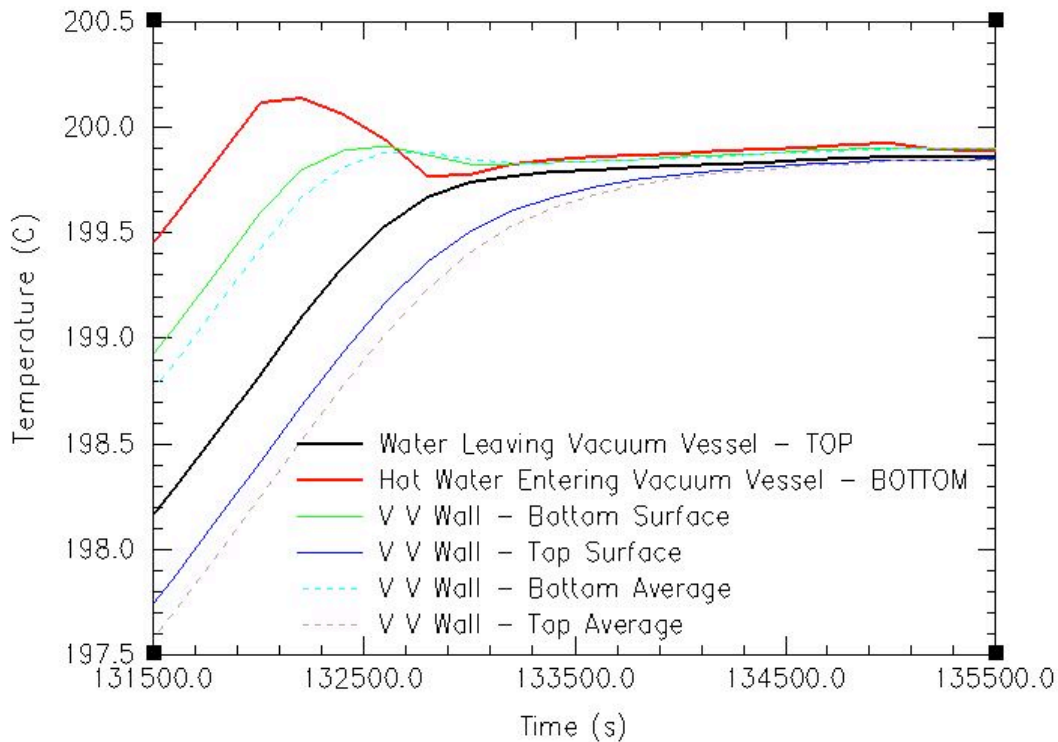


Fig. 10. Temperatures at the end of the baking transient.

9. DECAY HEAT MODEL

The decay heat loop has the model of the small decay heat pump incorporated for a flow of 40 kg/s. The same steam pressurizer described in Sect. 3 is used in this model, but the pressurizer controls are deactivated because this decay heat run will take place after a loss of power in the system. Only the decay heat pump and the pump in the secondary side of the decay heat HX run with emergency power. This model does not have temperature controls for the cold water returning to the VV. The decay heat model has additional structures modeling the FW/BLK, divertor, and thermal shield. Radiation models among these structures and from the last BLK and divertor structure to the VV walls are also incorporated in this model, exactly as in the previous model (Ref. 1).

10. REFERENCES

1. Juan J. Carbajo, Graydon L. Yoder, and Seokho H. Kim, *RELAP5 Model of the Vacuum Vessel Primary Heat Transfer System*, ITER Report 12103-TD0002-R00, May 2010.
2. Emilian Popov, Graydon L. Yoder, and Seokho H. Kim, *RELAP5 Model of the First Wall/Blanket Primary Heat Transfer System*, ITER Report 12101-TD0001-R00, June 2010.

INTERNAL DISTRIBUTION

- | | |
|------------------|----------------------|
| 1. J. B. Berry | 5. A. Y. Petrov |
| 2. J. J. Carbajo | 6. K. L. Wilcher |
| 3. J. J. Ferrada | 7. G. L. Yoder, Jr. |
| 4. S. H. Kim | 8. File-USIPO DCC-RC |

EXTERNAL DISTRIBUTION

10. K. P. Chang, ITER International Office, St. Paul Lez Durance Cedex, France 13607
11. W. Curd, ITER International Office, St. Paul Lez Durance Cedex, France 13607
12. G. Dell'Orco, ITER International Office, St. Paul Lez Durance Cedex, France 13607
13. K. Ioki, ITER International Office, St. Paul Lez Durance Cedex, France 13607
14. F. Li, ITER International Office, St. Paul Lez Durance Cedex, France 13607
15. Y. Udit, ITER International Office, St. Paul Lez Durance Cedex, France 13607